COMPUTER-CONTROLLED INFRARED MICROSCOPE FOR THERMAL ANALYSIS OF MICROWAVE TRANSISTORS

F. N. Sechi, B. S. Perlman, J. M. Cusack
RCA Corporation
David Sarnoff Research Center
Route 1
Princeton, New Jersey 08540

Abstract

A new technique for acquiring the temperature profile of microwave power transistors by infrared scanning has been developed. It provides for emissivity calibration using an infrared microscope interfaced with a computer.

Introduction

Microwave power transistors are small in size, and operate with high power densities, in the order of 10 KW/cm^2. Although the knowledge of the operating temperature of the device is particularly important as many of its characteristics, such as second-breakdown safe area, reliability, saturation and efficiency are functions of the highest temperature as well as the uniformity of the temperature profile, accurate temperature measurements are uncommon. The reason is that most of the measurement techniques developed for semiconductor devices are either complicated, unprecise or not quite applicable to microwave devices. For instance the covering of the device with temperature sensitive substances, like a thermographic phosphors[1] or liquid crystals is not acceptable, as these coatings affect the rf performance of the device. More sophisticated techniques, based either on the temperature dependance of the population of electrons-holes pairs photogenerated by a scanning laser beam[2] or on the recombination radiation of free minority carriers by doping atoms[3], can provide excellent spatial resolution but are difficult to implement. On the other hand, the simplest and most used technique, based on monitoring a temperature dependent parameter in the transistor[4], has been known to provide results that often correlate poorly with results obtained by different techniques[5].

The technique that is presently most convenient and accurate is based on the detection, by means of an infrared microscope, of the radiation thermally generated at the surface of the device. The major problem with such approaches is that different materials have different emissivity, thus a simple scan of a surface comprised of different materials - such as gold, silicon, oxides or aluminum - does not yield information readily usable. To work around this problem, researchers often coat the device surface with a compount opaque to the infrared radiation. This approach, however, can lead to problems, including distorted electrical performance and the inability to see the specific area under analysis through the microscope.

The new technique, presented in this paper, provides for emissivity calibration and two-dimensional scanning using an infrared microscope interfaced with, and under the control of, a computer system. The measurement of both surface emissivity and radiation allows to compute the surface temperature. Temperature profiles of the device are then presented graphically, either on a hard-copy plotter or a TV-type display.

Measurement System

A simplified functional diagram of the infrared microscope (Barnes Engineering model RM-24) is depicted in Fig. 1. A visible and an infrared (IR) channel allow the simultaneous measurement and viewing of the device under test. The indium-antimonide detector is cooled at -194°C by liquid nitrogen. An output signal, proportional to the amount of infrared radiation impinging on the detector is derived by low-noise amplification of the very low output-signal from the detector. The optical resolution of the instrument (diameter of the measuring dot) is 0.4 to 1.4 mils depending on the objective used.

The regular manually-controlled platform of the microscope was modified by adding a precision motor-driven mechanism. Figure 2 shows the x-y platform equipped with two precision stepping motors. The motors drive the micrometers through steel reinforced belts. The mechanism is virtually back-lash free, has a mechanical resolution of 1/16 mil (1 step of a motor) and a reset error lower than 2 μm. This resettability is excellent and is a very important factor for proper operation of the system. A built in heater element is used to raise the temperature of the top surface of the platform up to 200°C, while an invar structure maintains the surface stationary during changes in temperature.

Figure 3 is the system diagram of the computer-controlled infrared microscope. A control unit contains the electronic circuitry required to drive the stepping motors; each monitor features 200 steps per revolution. The step by step rotation is obtained by sequentially switching the currents in the four windings of the motor. The control circuits are such to provide a one-step rotation in either direction for any one pulse applied at an input port. These pulses are supplied by two computer controlled burst-pulse generators located in the multiprogrammer (HP6940). The control unit contains also a temperature controller that powers a heater imbedded in the substage platform, the temperature being monitored by means of a thermocouple. A D/A converter, also located in the multiprogrammer, programs the controller to set the wanted temperature on the platform. A scanning DVM measures the infrared radiation signal as well as the temperature of the platform.

The computer system, an HP-2100 minicomputer operating as part of a Real Time Executive (RTE) system, controls the operation of the overall system. This multitasking computer system is shared with other automatic measurement set-ups and other computational programs. A hard-copy plotter and a TV monitor are used for displaying the thermal profiles of the device under test.

For the measurement of temperature profiles, the device biased for normal operating conditions, is mounted on the x-y motorized platform and is scanned along the wanted pattern. Infrared radiation is measured at discrete points of the surface. The high mechanical resolution of the system allows to analyze up to 16 points per each mil of distance. The emissivity is then measured by rescanning the device turned off and heated uniformly at a specified elevated temperature. Although in principle this would yield sufficient information for determining the emissivity of each point on the surface, for improved accuracy the procedure is repeated two more times at different temperatures. Having stored all the measured data in a disc file, a curve is fitted through the calibration data for each measured point on the surface. The temperature of that point is then computed from the measured radiation. Finally temperature profiles of the device are automatically plotted or displayed on the TV monitor.

An algorithm based on the fitting of a 2nd order polynomial through the calibration point is used in this system when interpolation is required. This results in computational simplicity and speed. When extrapolation is required, a second algorithm is used, based on a more accurate formulation of the radiation output voltage as function of temperature. The computation is more lengthy but allows the calibration to be performed at temperatures lower than the operating temperature of the device, which is convenient when the device, and sometimes the surrounding structure, cannot be heated at high temperatures. The expression, relating radiation to temperature, was derived by integrating over a range of wavelengths the spectral emission of a body at temperature T(Plank's law)

$$\frac{\partial H}{\partial \lambda} = \frac{C_1}{\lambda^5} \frac{1}{e^{C_2/\lambda T} - 1} \qquad (1)$$

H = power per unit area

λ = wavelength (μm)

C_1, C_2 = constants

times the responsivity of the detector, approximated by an experimental function of λ:

$$R \propto e^{0.368\lambda} \qquad (2)$$

The result is the following equation:

$$E(T) = A\varepsilon\left(B + \frac{C}{T}\right) e^{-\frac{D}{T}} - F \qquad (3)$$

where: E(T) = radiation output voltage
T = temperature (°K)
ε = emissivity
A = constant related to the gain of the amplifier
B = 0.3, C = 533, D = 3.55 10^3

and F is equal to the first term of equation 3 computed for ε=1 and T=Ta=ambient temperature:

$$F = A\left(B + \frac{C}{Ta}\right) e^{-\frac{D}{Ta}} \qquad (4)$$

Test Results

The temperature profile of a 3 cell high power bipolar transistor, that is capable of providing 7.5W CW at GHz, is shown in Fig. 5. Since the purpose of the test was to analyze the quality of the bond between the pellet (collector) and the carrier, a low voltage (5V) high current (1.5A) DC supply was used to bias the device. The profiles show excellent temperature uniformity between the cells, with the center cell only slightly hotter than the two side-ones, as expected. The temperature profile of a similar device, having a defective joint between the pellet and the carrier, is shown in Fig. 6. Not only is one of the side cells much hotter than the other two, but also its operating temperature is 80°C higher than that of the first transistor, although dissipating the same amount of power. The problem was later traced to a defective metallization on the carrier.

Useful information has also been obtained from thermal scans of high power GaAs FETs. One such device, capable of providing 1W of output power at X-band, is shown in Fig. 7. The GaAs pellet is flip-chip mounted with its eleven sources bonded to a Cu heatsink. This construction provides both excellent heatsinking for the pellet and the necessary low-inductance connection of the sources to the ground. By taking advantage of the low attenuation of infrared radiation (λ=5μm) through GaAs, it is possible to measure the temperature of the surface close to the active area of the device. Good bonding of the surface pads to the carrier results in a low and uniform temperature profile, as shown in Fig. 7. The temperature dips over each source pad, as these pads are also heatsinks.

The temperature profile of a device with a defective source bonding is shown in Fig. 8. Although all the sources are electrically connected, the thermal contact is not uniform, which results in a degradation of the RF performance and in low reliability.

Conclusions

By providing the means for automatic data acquisition and control for an otherwise manual infrared microscope, the task of recording accurate thermal maps of microwave transistors has been simplified dramatically. The primary advantage of this approach, over noncomputerized methods, is the ability of the computer to compensate for variations in surface emissivity by systematically recording radiation from the unknown structure at several preset calibration temperatures. Radiation from a "live" device can then be converted to actual temperature and plotted automatically. A conservative estimate of the accuracy of this method is $\pm$1°C. This technique is remarkably effective in the study and diagnosis of microwave power transistors, because high or non-uniform temperatures often can be correlated with poor transistor performance.

Acknowledgements

The authors wish to thank D. Fairbanks for the many useful suggestions in regard to the mechanical drive of the platform, R. Paglione and L. Mackey for their help in the mechanical design and W. Haldane for the electrical assembly of the control circuit. Appreciation is also expressed to Dr. E. Belohoubek for the many technical discussions.

References

1. D. S. Brenner, "A Technique for Measuring the Surface Temperature of Transistors by Means of Fluorescent Phosphors," NBS Tech. Note 591, July, 1971.

2. D. Sawyer, D. Berning, "Laser Scanning of Active Semiconductor Devices," NBS Special Publication 400-27, February 1976.

3. Y. P. Varshui, "Band-to-Band Recombination in Groups IV, VI, and II-V Semiconductors (I)," Physica Status Solidi, Vol. 19, pp. 459-514, February, 1967.

4. F. Oettinger et al. "Thermal Characterization of Power Transistors," IEEE Trans. on Electron Devices, Vol. ED23, No. 8, August, 1976, pp. 831-838.

5. L. Walshak, E. Poole, "Thermal Resistance Measurement by IR Scanning," Microwave Journal, February, 1977, pp. 62-65.

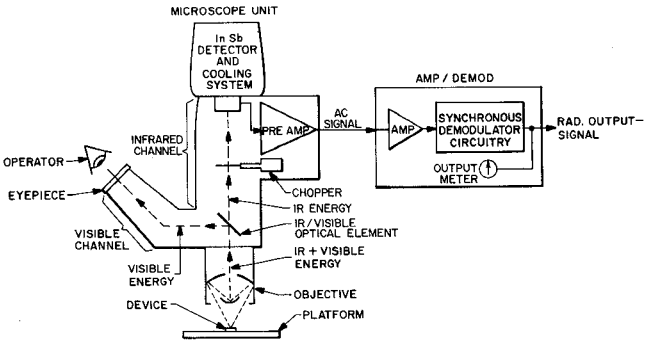

Figure 1. Functional diagram of infrared microscope (Barnes Engineering Mod. RM2a)

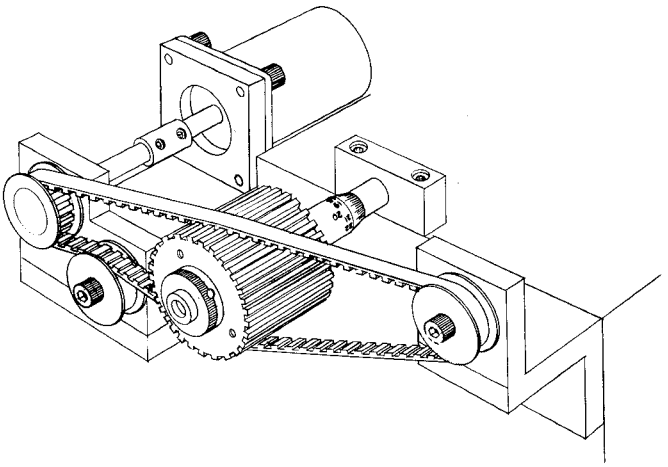

Figure 2. Platform with stepping motors

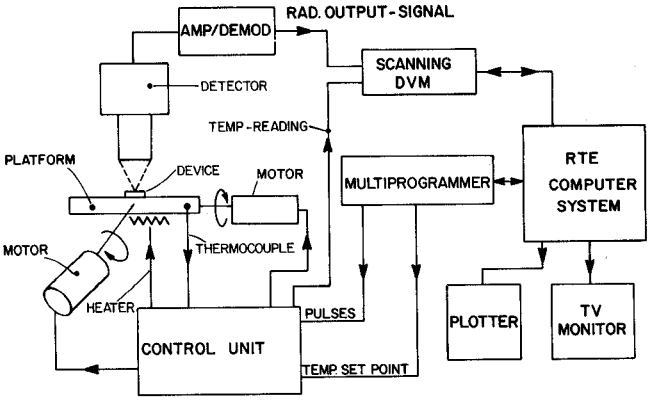

Figure 3. System diagram of computer-controlled infrared microscope

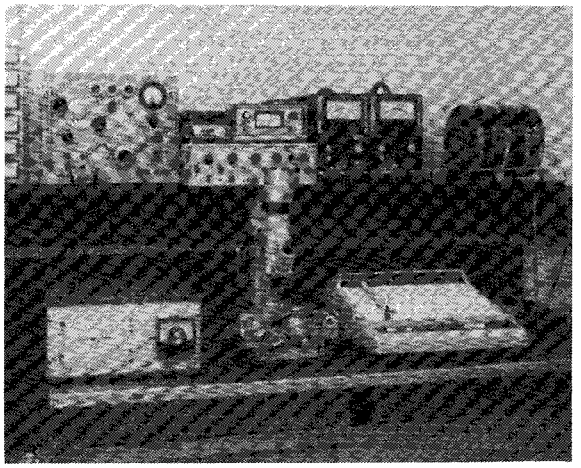

Figure 4. Computer-controlled infrared microscope

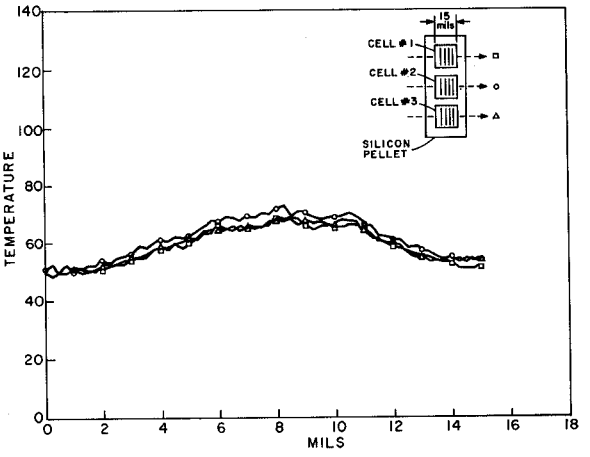

Figure 5. Temperature profile of a bipolar transistor having a good heatsink

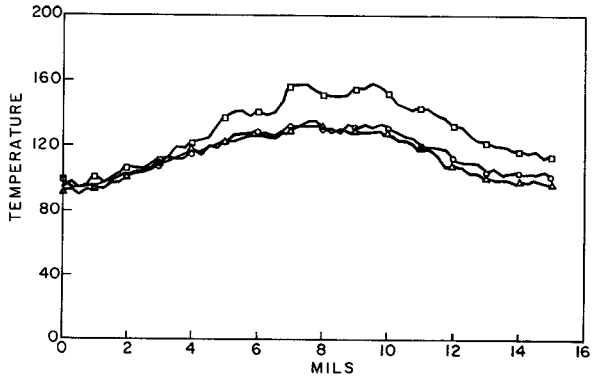

Figure 6. Temperature profile of a bipolar transistor having a defective heatsink

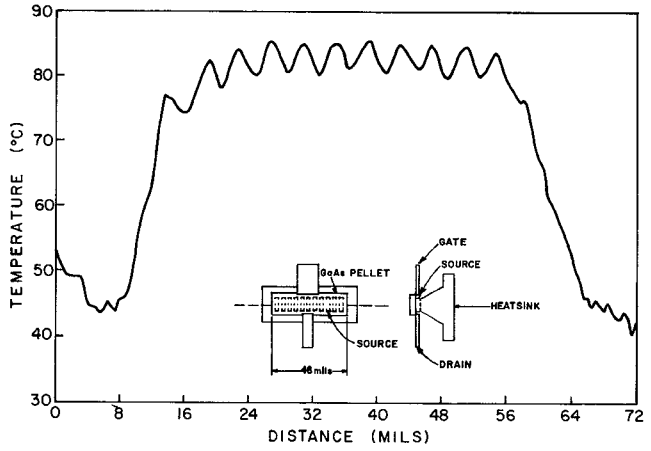

Figure 7. Temperature profile of an FET having a good heatsink

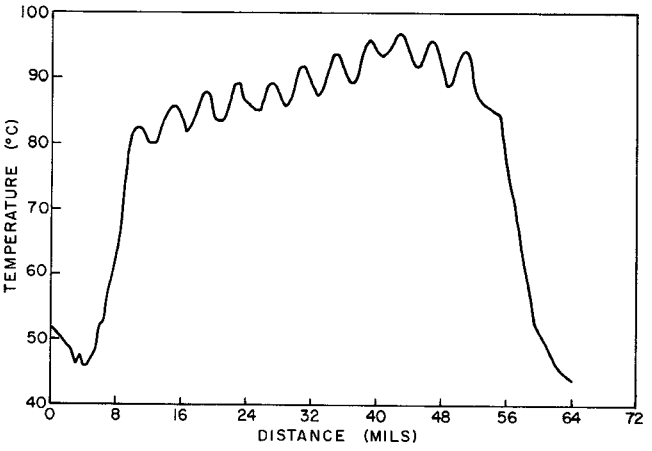

Figure 8. Temperature profile of an FET having a defective heatsink